

Calculations of Isotope Effects in Elimination Reactions. New Experimental Criteria for Tunneling in Slow Proton Transfers¹

William H. Saunders, Jr.

Contribution from the Department of Chemistry, University of Rochester, Rochester, New York 14627. Received July 30, 1984

Abstract: Isotope-effect calculations have been carried out on the model reaction $\text{CCH}_2\text{CH}_2\text{Cl} + \text{OH}^- \rightarrow \text{CCH}=\text{CH}_2 + \text{Cl}^- + \text{H}_2\text{O}$. When the bending motions of the nontransferred β -hydrogen are coupled with the stretching motion of the transferred β -hydrogen, a tunnel correction to the secondary β -hydrogen isotope effect is introduced. The kinetic secondary effect can be larger than the equilibrium secondary effect, in agreement with recent experiments. The contribution of tunneling to the secondary kinetic effect decreases with increased mass of the transferred atom. Deviations from the expected relation between deuterium and tritium isotope effects, both primary and secondary, can occur when tunneling is important, and are large enough to observe easily when $k_{\text{H}}/k_{\text{D}}$ (or $k_{\text{H}}/k_{\text{T}}$) calculated from $k_{\text{D}}/k_{\text{T}}$ is compared with directly calculated $k_{\text{H}}/k_{\text{D}}$ (or $k_{\text{H}}/k_{\text{T}}$). Deuterium substitution at the β -carbon also reduces the contribution of tunneling to β -carbon isotope effects. Tunneling causes a decrease in the ratio of Arrhenius preexponential factors, $A_{\text{light}}/A_{\text{heavy}}$, not only for primary hydrogen isotope effects but also for secondary hydrogen isotope effects and carbon isotope effects. The ratio increases again when the mass of the transferred atom increases. Deviations from the rule of the geometric mean can be expected when isotopic substitution at one position affects the contribution of tunneling to the isotope effect at another. These predictions provide new experimental tests for tunneling in slow proton transfers.

Primary deuterium and tritium isotope effects in slow proton transfers have been extensively studied, but much less attention has been given to the secondary isotope effects incurred when a nontransferred hydrogen on the donor atom is replaced by deuterium or tritium. Whether the primary and secondary effects are cumulative has remained until recently almost completely unknown.

A reasonable a priori assumption is that the secondary isotope effect should reflect bonding changes at the donor atom in the transition state, which in most cases means a change in hybridization. By this line of reasoning, the secondary kinetic isotope effect is expected to vary monotonically from a small value for a reactant-like transition state to a near-equilibrium value for a product-like transition state. Recent work has shown, however, that secondary kinetic isotope effects in hydride transfers can significantly exceed the equilibrium effects.²⁻⁴ Similar results are reported for elimination reactions of 2-arylethyl derivatives,⁵ where the kinetic secondary tritium isotope effects often exceed the equilibrium effects estimated from the fractionation factors of Hartshorn and Shiner.⁶

Model calculation on the hydride transfer reaction by Huskey and Schowen⁷ showed that the kinetic secondary isotope effects could be made to exceed the equilibrium isotope effects when the motion of the nontransferred hydrogen was coupled with that of the transferred hydrogen, thereby introducing a tunnel correction to the kinetic secondary isotope effect. Calculations by Saunders⁸ on a model for the bimolecular (E2) elimination reaction similarly predicted a tunnel correction to the kinetic secondary isotope effect when the stretching motion of the transferred hydrogen was coupled with bending motions of the nontransferred hydrogen. The present paper gives a more complete account of these calculations and predicts that substrates with multiple isotopic

substitution will show measurable deviations from cumulative behavior of the primary and secondary isotope effects when tunneling is significant.

The Model

The model (eq 1) was very similar to that used in earlier calculations.⁹ Bond lengths, diagonal force constants, and the



manner in which force constants involving reacting bonds vary with bond orders were all identical with those tabulated earlier⁹ and will not be repeated here. Synchronous changes in all reacting bonds were assumed, and total bond order to a given atom was conserved. Thus, when n_{OH} (the bond order of the HO---H bond) was 0.3, n_{CH} was 0.7, n_{CC} 1.3, and n_{CCl} 0.7. The geometry at the α and β carbon atoms varied linearly from tetrahedral to trigonal as n_{OH} varied from 0 to 1. Chlorine was used as the leaving group in all cases, because the earlier calculations⁹ had shown that the nature of the leaving group, other parameters being equal, had a negligible influence on the primary and secondary isotope effects at the β -position.

Off-diagonal force constants were assigned as before so as to ensure a reaction coordinate motion with reacting bond lengths changing in such a way as to convert reactants smoothly to products. The formalism by which this is accomplished involved defining the determinant of the F matrix by eq 2, substituting in

$$|F| = DF_{11} \cdots F_{nn} \quad (2)$$

it off-diagonal elements defined by eq 3-6, and expanding it to give eq 7. When $C = 0$, eq 7 becomes eq 8, the same relation

$$F_{ij} = F_{ji} = K(F_{ii}F_{jj})^{1/2} \quad (3)$$

$$K = A \text{ for O---H, C---H} \quad (4)$$

$$K = B \text{ for C---H, C=C and C=C, C---Cl} \quad (5)$$

$$K = C \text{ for C---H, C---C---H; C---H, C=C---H; and C---H, H---C---H} \quad (6)$$

$$1 - A^2 - 2B^2 - C^2 + A^2B^2 - B^2C^2 = D \quad (7)$$

used before.⁹ The parameters A, B, and C represent the strength

$$1 - 2B^2 - A^2 + A^2B^2 = D \quad (8)$$

(1) This work was supported by the National Science Foundation.

(2) Kurz, L. C.; Frieden, C. *J. Am. Chem. Soc.* **1980**, *102*, 4198-4203.

(3) Cook, P. F.; Oppenheimer, N. J.; Cleland, W. W. *Biochemistry* **1981**, *20*, 1817-1825. Cook, P. F.; Blanchard, J. S.; Cleland, W. W. *Ibid.* **1980**, *19*, 4853-4858. Cook, P. F.; Cleland, W. W. *Ibid.* **1981**, *20*, 1797-1805, 1905-1916.

(4) Ostović, D.; Roberts, M. G.; Kreevoy, M. M. *J. Am. Chem. Soc.* **1983**, *105*, 7629-7631.

(5) Subramanian, Rm.; Saunders, W. H., Jr. *J. Am. Chem. Soc.*, in press.

(6) Buddenbaum, W. E.; Shiner, V. J., Jr. In "Isotope Effects on Enzyme-Catalyzed Reactions"; Cleland, W. W., O'Leary, M. H., Northrop, D. B., Eds.; University Park Press: Baltimore, 1977; p 11. Hartshorn, S. R.; Shiner, V. J., Jr. *J. Am. Chem. Soc.* **1972**, *94*, 9002-9012.

(7) Huskey, W. P.; Schowen, R. L. *J. Am. Chem. Soc.* **1983**, *105*, 5704-5706.

(8) Saunders, W. H., Jr. *J. Am. Chem. Soc.* **1984**, *106*, 2223-2224.

(9) Saunders, W. H. *Chem. Scr.* **1975**, *8*, 27-36; **1976**, *10*, 82-89. Katz, A. M.; Saunders, W. H., Jr. *J. Am. Chem. Soc.* **1969**, *91*, 4469-4472.

Table I. Parameters for Off-Diagonal F Matrix Elements^a

model	A	B	C ^b	D
1	1.05	0.33	0	-0.20
3	1.00	0.44-0.35	0.28	-0.20
4	1.00	0.52-0.26	0.49	-0.30
5	1.00	0.56-0.22	0.57	-0.35

^a For definitions, see text and eq 2-9. ^b C was negative for the H--C, C--C--H and H--C, C=C--H coupling and positive for the H--C, H--C--H coupling.

of coupling between the vibrational motions involved, while D is the curvature parameter. The more negative D is, the greater the curvature of the potential surface in the vicinity of the transition state, and the more tunneling contributes to the rates and isotope effects.

One additional refinement was introduced. If C is defined by eq 9, the off-diagonal elements it controls vanish at both $n_{OH} = 0$ and $n_{OH} = 1$ (the latter because $F_{C--H} = 0$). The parameters A and D were held constant while B varied compensatingly so as to satisfy eq 7.

$$C = C'n_{OH}^{1/2} \quad (9)$$

The parameters used are listed in Table I. Those for model 1 are the same as were used in most of the earlier calculations, where they were shown to give reasonable values of all isotope effects. Models 1, 3, 4, and 5 all let force constants for the HC--H, CC--H, CC--Cl, and HC--Cl bends approach constant values for product-like transition states thereby simulating the out-of-plane bends of the atoms attached to the sp²-hybridized carbons of the product. No model 2 is listed because that model, which let these bending force constants approach zero, was found in the earlier work to give unrealistically large equilibrium secondary isotope effects.⁸ Numbering of the models was left unchanged in the present work so as to facilitate comparison with ref 8.

Qualitatively all models have similar contributions of proton transfer to the reaction coordinate motion ($A = 1.0-1.05$). In model 1 the C--H stretch is not coupled to the bending motions of the nontransferred hydrogen, while such coupling is present to a steadily increasing extent in models 3, 4, and 5. Models 4 and 5 also have larger curvature parameters and can be expected to show larger tunnel corrections as a result. These models were chosen out of a considerable number tried because they gave reasonable values of both primary and secondary isotope effects. Model 4 gives secondary isotope effects close to the largest experimentally obtained to date.⁵

The calculations were performed with use of the BEBOVIB-IV program.¹⁰ Tunnel corrections were calculated from the first term of the Bell equation (eq 10),¹¹ with the tunneling frequency $\nu_t =$

$$Q_t = 0.5u_t/\sin(0.5u_t) \quad (10)$$

$|\nu_L^*|$, the absolute value of the reaction coordinate frequency. The results on deuterium, tritium, ¹³C, and ¹⁴C isotope effects are given in Tables II-IV. The tables quote isotope effects at 45 °C, because that is close to the temperature used in our experiments,⁵ but calculations were also done at 25, 35, and 55 °C. All isotope effects include the tunnel correction except when a subscript sc indicates that the effect is "semiclassical" (all factors except the tunnel correction). Primary and secondary effects are differentiated by showing the former as subscripts and the latter as superscripts. Thus, the primary H/D effect is k_H^H/k_D^H and the secondary effect is k_H^H/k_D^D , both for a singly labeled substrate. The expression $k_D^D/k_{D(13)}^D$ denotes a reaction in which both substrates are doubly labeled at the β -position with deuterium and one with ¹³C as well. The Arrhenius parameters quoted in Tables VI and

VII were obtained by fitting the calculated results to the Arrhenius equation at 25, 35, 45, and 55 °C with use of a standard least-squares program.

Results and Discussion

Table II shows that all models give reasonable primary isotope effects (k_H^H/k_D^H and k_H^H/k_T^H), and the tunnel corrections to the primary isotope effects are comparable to those obtained experimentally.¹²⁻¹⁴ The semiclassical secondary isotope effects all increase monotonically with n_{OH} toward values close to the equilibrium secondary isotope effects calculated from fractionation factors ($K_H^H/K_D^D = 1.124$ at 25 °C, corresponding to 1.115 at 45 °C and to $K_H^H/K_T^T = 1.170$ at 45 °C).^{6,8} Similar monotonic increases are found for the full secondary isotope effects with model 1, which lacks stretch-bend coupling. When such coupling is introduced, an appreciable contribution of tunneling to the secondary isotope effects appears (model 3). With increased coupling (models 4 and 5), tunneling becomes a dominant contribution to the full secondary isotope effects in the region $n_{OH} = 0.3-0.5$, resulting in k_H^H/k_D^D values that exceed the equilibrium effects. Model 4 gives k_H^H/k_D^D values corresponding rather closely to the largest experimental values.⁵

One could argue that a similar dependence of k_H^H/k_D^D on n_{OH} might be generated without recourse to tunneling if the transition states near the half-transfer point were loose, with $n_{OH} + n_{CH} < 1$. A variant of model 1 in which $n_{OH} = n_{CH} = 0.2$ produced an increase in $(k_H^H/k_D^D)_{sc}$, but the effect still failed to exceed the equilibrium value. It seemed unrealistic to expect sacrifice of more than half of the bonding to the proton in transit in a real system, so such models were not explored further.

Both deuterium and tritium isotope effects were calculated to facilitate comparison with experimental results and to explore the relationship between effects with the two isotopes. If hydrogen isotope effects are assumed to result only from zero-point energy effects, eq 11 can be derived.^{15,16} For the conversion of k_H/k_D

$$\frac{\ln(k_1/k_2)_{sc}}{\ln(k_1/k_3)_{sc}} = \frac{1 - (m_1/m_2)^{1/2}}{1 - (m_1/m_3)^{1/2}} \quad (11)$$

to k_H/k_T , the factor on the right side is 1.44 for $m_H:m_D:m_T$ in the ratio 1:2:3, or 1.43 if they are in the ratio of the reduced masses of ¹²C-H:¹²C-D:¹²C-T.¹⁷ It was at one time hoped that deviations from eq 11 might be diagnostic for tunneling, but Lewis and Robinson pointed out that such deviations should be small unless tunneling was quite extensive.¹⁸ Model calculations also predict deviations to be small.¹⁹

The relation holds very well for the semiclassical isotope effects, both primary (column 7 of Table II vs. column 3 of Table V) and secondary (column 9 of Table II vs. column 5 of Table V). The full secondary isotope effects still obey eq 11 within ca. 2% (column 10 of Table II vs. column 6 of Table V). Noticeable deviations occur with the primary effects (column 8 of Table II vs. column 4 of Table V), especially with models 4 and 5. The values from eq 11 run larger than the directly calculated k_H^H/k_D^D values because the tunnel corrections run $Q_{tH} > Q_{tD} > Q_{tT}$. The worst deviations, however, are barely over 10%. Careful experiments and a (probably unjustified) faith that 1.44 is just the right factor to

(12) Kaldor, S. B.; Saunders, W. H., Jr. *J. Am. Chem. Soc.* **1979**, *101*, 7594-7599.

(13) Kaldor, S. B.; Fredenburg, M. E.; Saunders, W. H., Jr. *J. Am. Chem. Soc.* **1980**, *102*, 6296-6299.

(14) Miller, D. J.; Saunders, W. H., Jr. *J. Org. Chem.* **1981**, *46*, 4247-4252.

(15) Melander, L.; Saunders, W. H., Jr. "Reaction Rates of Isotopic Molecules"; Wiley: New York, 1980; pp 28-29, 143-144.

(16) Swain, C. G.; Stivers, E. C.; Reuwer, J. F., Jr.; Schaad, L. J. *J. Am. Chem. Soc.* **1958**, *80*, 5885-5893.

(17) Streitwieser, A., Jr.; Hollyhead, W. B.; Pudjaatmaka, A. H.; Owens, N. H.; Kruger, T. L.; Rubenstein, P. A.; MacQuarrie, R. A.; Brokaw, M. L.; Chu, W. K. C.; Niemeyer, H. M. *J. Am. Chem. Soc.* **1971**, *93*, 5088-5096.

(18) Lewis, E. S.; Robinson, J. K. *J. Am. Chem. Soc.* **1968**, *90*, 4337-4344.

(19) Stern, M. J.; Weston, R. E., Jr. *J. Chem. Phys.* **1974**, *60*, 2815-2821.

(10) Sims, L. B.; Burton, G.; Lewis, D. E. Bebovib IV, Quantum Chemistry Program Exchange, Department of Chemistry, Indiana University, Bloomington, Indiana 47401, Program No. 337.

(11) Bell, R. P. "The Tunnel Effect in Chemistry"; Chapman and Hall: New York, 1980; pp 60-63.

Table II. Primary and Secondary Deuterium and Tritium Isotope Effects for HO⁻ + CCH₂CH₂Cl at 45 °C (Singly Labeled Substrates^{a,b})

model	n_{OH}	$(k_{\text{H}}^{\text{H}}/k_{\text{D}}^{\text{H}})_{\text{sc}}$	$k_{\text{H}}^{\text{H}}/k_{\text{D}}^{\text{H}}$	$(k_{\text{H}}^{\text{H}}/k_{\text{H}}^{\text{D}})_{\text{sc}}$	$k_{\text{H}}^{\text{H}}/k_{\text{H}}^{\text{D}}$	$(k_{\text{H}}^{\text{H}}/k_{\text{T}}^{\text{H}})_{\text{sc}}$	$k_{\text{H}}^{\text{H}}/k_{\text{T}}^{\text{H}}$	$(k_{\text{H}}^{\text{H}}/k_{\text{H}}^{\text{T}})_{\text{sc}}$	$k_{\text{H}}^{\text{H}}/k_{\text{H}}^{\text{T}}$
1	0.1	2.718	2.759	1.014	1.016	4.261	4.370	1.022	1.025
	0.3	5.051	7.400	1.025	1.027	10.194	16.950	1.033	1.037
	0.5	5.034	7.074	1.048	1.053	10.146	16.051	1.067	1.074
	0.7	3.393	3.568	1.082	1.086	5.864	6.344	1.112	1.118
	0.9	1.790	1.794	1.113	1.113	2.326	2.335	1.158	1.158
3	0.1	2.573	2.628	1.027	1.032	3.949	4.087	1.042	1.051
	0.3	4.384	6.119	1.032	1.069	8.316	13.134	1.042	1.098
	0.5	4.300	5.742	1.058	1.088	8.087	12.099	1.077	1.123
	0.7	3.017	3.177	1.088	1.093	4.947	5.371	1.120	1.128
	0.9	1.715	1.719	1.103	1.103	2.184	2.194	1.140	1.410
4	0.1	2.632	2.789	1.037	1.055	4.072	4.464	1.057	1.084
	0.3	4.069	7.508	1.031	1.184	7.419	16.833	1.038	1.266
	0.5	4.020	6.665	1.056	1.197	7.272	14.490	1.073	1.283
	0.7	2.972	3.274	1.107	1.142	4.796	5.580	1.148	1.202
	0.9	1.712	1.721	1.110	1.111	2.174	2.196	1.151	1.153
5	0.1	2.643	2.874	1.038	1.064	4.088	4.660	1.056	1.097
	0.3	3.959	8.757	1.027	1.270	7.110	20.187	1.032	1.392
	0.5	3.929	7.379	1.052	1.267	7.013	16.337	1.067	1.385
	0.7	2.956	3.328	1.110	1.162	4.745	5.703	1.152	1.232
	0.9	1.711	1.722	1.114	1.115	2.170	2.197	1.158	1.160

^aSee Table I and the text for descriptions of the models. ^bSubscripts D or T refer to the primary and superscripts D or T to the secondary isotope effect. Subscript sc refers to the semiclassical (without tunneling) isotope effect.

Table III. Primary and Secondary Deuterium and Tritium Isotope Effects for HO⁻ + CCH₂CH₂Cl at 45 °C (Doubly Labeled Substrates^{a,b})

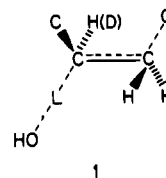
model	n_{OH}	$(k_{\text{D}}^{\text{H}}/k_{\text{D}}^{\text{D}})_{\text{sc}}$	$k_{\text{D}}^{\text{H}}/k_{\text{D}}^{\text{D}}$	$(k_{\text{T}}^{\text{H}}/k_{\text{T}}^{\text{D}})_{\text{sc}}$	$k_{\text{T}}^{\text{H}}/k_{\text{T}}^{\text{D}}$	$(k_{\text{D}}^{\text{D}}/k_{\text{D}}^{\text{T}})_{\text{sc}}$	$k_{\text{D}}^{\text{D}}/k_{\text{D}}^{\text{T}}$	$(k_{\text{D}}^{\text{D}}/k_{\text{T}}^{\text{D}})_{\text{sc}}$	$k_{\text{D}}^{\text{D}}/k_{\text{T}}^{\text{D}}$
1	0.1	1.013	1.014	1.012	1.012	1.006	1.007	1.567	1.582
	0.3	1.030	1.031	1.032	1.033	1.010	1.011	2.022	2.295
	0.5	1.056	1.059	1.060	1.063	1.019	1.021	2.023	2.276
	0.7	1.091	1.094	1.096	1.098	1.032	1.034	1.735	1.784
	0.9	1.123	1.123	1.127	1.127	1.044	1.045	1.304	1.306
3	0.1	1.021	1.024	1.017	1.019	1.011	1.014	1.529	1.548
	0.3	1.037	1.052	1.038	1.046	1.013	1.021	1.898	2.134
	0.5	1.064	1.078	1.066	1.074	1.022	1.029	1.884	2.099
	0.7	1.092	1.096	1.094	1.096	1.032	1.034	1.642	1.692
	0.9	1.113	1.113	1.117	1.117	1.038	1.038	1.279	1.281
4	0.1	1.029	1.039	1.024	1.030	1.014	1.020	1.540	1.588
	0.3	1.043	1.104	1.046	1.083	1.014	1.043	1.829	2.200
	0.5	1.070	1.134	1.075	1.117	1.024	1.052	1.817	2.141
	0.7	1.110	1.134	1.111	1.129	1.040	1.051	1.615	1.697
	0.9	1.119	1.120	1.123	1.124	1.041	1.042	1.275	1.280
5	0.1	1.030	1.044	1.025	1.035	1.014	1.023	1.539	1.606
	0.3	1.042	1.129	1.047	1.099	1.013	1.052	1.804	2.245
	0.5	1.069	1.161	1.076	1.135	1.022	1.062	1.796	2.171
	0.7	1.114	1.149	1.115	1.142	1.041	1.057	1.607	1.703
	0.9	1.123	1.124	1.127	1.128	1.043	1.044	1.273	1.279

^{a,b}See corresponding footnotes to Table II.

use in eq 11 would be needed to use these deviations to detect tunneling.

The temperature dependence of the isotope effect is more useful as a measure of tunneling. Low ratios of the Arrhenius pre-exponential factors ($A_{\text{H}}/A_{\text{D}}$ and $A_{\text{H}}/A_{\text{T}}$) have for some time been taken as reliable evidence of tunneling contributions to primary isotope effects.²⁰ The values in columns 3 and 5 of Table VI are comparable to those obtained experimentally in elimination reactions.¹²⁻¹⁴ The present work shows that the $A_{\text{H}}/A_{\text{D}}$ and $A_{\text{H}}/A_{\text{T}}$ ratios for the secondary isotope effects behave in an analogous manner. Examination of columns 7 and 9 of Table VI shows that $A_{\text{H}}/A_{\text{D}}$ and $A_{\text{H}}/A_{\text{T}}$ remain above 0.95 for model 1, in which there is little or no tunneling contribution to the secondary isotope effect, but can drop as low as 0.28 and 0.19 respectively, when tunneling is extensive (model 5). Even for model 4, the values of 0.5-0.6 at $n_{\text{OH}} = 0.3-0.5$ should be easily distinguishable experimentally from the near-unity values expected when tunneling is unimportant. We are currently studying the temperature dependence of $k_{\text{H}}^{\text{H}}/k_{\text{H}}^{\text{T}}$ values.

In the calculations of Huskey and Schowen on hydride transfer, it was noted that the secondary isotope effect decreased when the transferred atom was changed from protium to deuterium.⁷ We have explored more extensively the behavior of the secondary isotope effect in multiply labeled substrates. The model first chosen was 1, where the secondary H/D effect was calculated



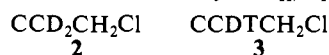
for L = H, D, and T. The semiclassical effects (column 5 of Table II and columns 3 and 5 of Table III) vary little. The small changes found are usually in the direction of $(k_{\text{L}}^{\text{H}}/k_{\text{L}}^{\text{D}})_{\text{sc}}$ increasing as the mass of L increases. The full secondary effects (column 6 of Table II and columns 4 and 6 of Table III), on the other hand, show decided decreases in $k_{\text{L}}^{\text{H}}/k_{\text{L}}^{\text{D}}$ for models 4 and 5, $n_{\text{OH}} = 0.3-0.5$, as L increases in mass.

Table IV. β -Carbon Isotope Effects for $\text{HO}^- + \text{CCH}_2\text{CH}_2\text{Cl}$ and $\text{CCD}_2\text{CH}_2\text{Cl}$ at 45 °C^{a-c}

model	n_{OH}	$(k_{\text{H}}^{\text{H}}/k_{\text{H}(13)}^{\text{H}})_{\text{sc}}$	$(k_{\text{D}}^{\text{D}}/k_{\text{D}(13)}^{\text{D}})_{\text{sc}}$	$k_{\text{H}}^{\text{H}}/k_{\text{H}(13)}^{\text{H}}$	$k_{\text{D}}^{\text{D}}/k_{\text{D}(13)}^{\text{D}}$	$(k_{\text{H}}^{\text{H}}/k_{\text{H}(14)}^{\text{H}})_{\text{sc}}$	$(k_{\text{D}}^{\text{D}}/k_{\text{D}(14)}^{\text{D}})_{\text{sc}}$	$k_{\text{H}}^{\text{H}}/k_{\text{H}(14)}^{\text{H}}$	$k_{\text{D}}^{\text{D}}/k_{\text{D}(14)}^{\text{D}}$
1	0.1	1.0027	1.0022	1.0037	1.0027	1.0052	1.0042	1.0072	1.0051
	0.3	0.9959	1.0002	1.0004	1.0018	0.9922	1.0003	1.0008	1.0034
	0.5	1.0004	1.0065	1.0121	1.0117	1.0006	1.0122	1.0229	1.0223
	0.7	1.0158	1.0184	1.0213	1.0217	1.0301	1.0350	1.0406	1.0414
	0.9	1.0155	1.0197	1.0158	1.0200	1.0293	1.0374	1.0299	1.0379
3	0.1	1.0069	1.0072	1.0081	1.0077	1.0132	1.0135	1.0154	1.0145
	0.3	1.0036	1.0084	1.0114	1.0119	1.0067	1.0157	1.0215	1.0225
	0.5	1.0078	1.0144	1.0244	1.0231	1.0146	1.0272	1.0463	1.0440
	0.7	1.0219	1.0255	1.0299	1.0311	1.0416	1.0486	1.0569	1.0594
	0.9	1.0196	1.0243	1.0201	1.0248	1.0371	1.0462	1.0381	1.0471
4	0.1	1.0107	1.0119	1.0132	1.0130	1.0202	1.0224	1.0251	1.0246
	0.3	1.0066	1.0129	1.0269	1.0217	1.0122	1.0242	1.0509	1.0412
	0.5	1.0075	1.0161	1.0403	1.0323	1.0139	1.0303	1.0765	1.0614
	0.7	1.0208	1.0264	1.0369	1.0375	1.0396	1.0503	1.0704	1.0717
	0.9	1.0250	1.0300	1.0268	1.0315	1.0476	1.0572	1.0509	1.0601
5	0.1	1.0125	1.0141	1.0162	1.0159	1.0236	1.0265	1.0308	1.0301
	0.3	1.0074	1.0143	1.0383	1.0263	1.0137	1.0267	1.0727	1.0498
	0.5	1.0073	1.0165	1.0505	1.0361	1.0134	1.0309	1.0960	1.0688
	0.7	1.0199	1.0262	1.0395	1.0395	1.0377	1.0498	1.0753	1.0756
	0.9	1.0263	1.0314	1.0287	1.0335	1.0501	1.0598	1.0546	1.0639

^{a,b}See corresponding footnotes to Table I. ^cSubscripts (13) or (14) indicate ¹³C or ¹⁴C, respectively, at the β -carbon atom.

Testing these predictions experimentally presents potential problems. Determination of $k_{\text{T}}^{\text{H}}/k_{\text{T}}^{\text{D}}$ would be particularly difficult. While $k_{\text{D}}^{\text{H}}/k_{\text{D}}^{\text{D}}$ would be easier, it would still require precise rate measurements on d_1 and d_2 species, along with precise deuterium analysis of the product from the d_1 species to separate k_{H}^{D} from k_{D}^{H} . An experimentally easier approach that gives comparable information is to start with a substrate doubly labeled with deuterium, **2**, and then tracer-label it with tritium. The result is a mixture of **2** and **3**. With such a mixture, $k_{\text{D}}^{\text{D}}/k_{\text{T}}^{\text{D}}$ and $k_{\text{D}}^{\text{D}}/k_{\text{T}}^{\text{D}}$ can be determined in the same way as $k_{\text{H}}^{\text{H}}/k_{\text{T}}^{\text{H}}$ and $k_{\text{H}}^{\text{H}}/k_{\text{T}}^{\text{H}}$.^{5,21}



Comparison of these D/T isotope effects with the more familiar H/D and H/T effects must be made via eq 11. From eq 11, the appropriate relations are eq 12 and 13, assuming $m_{\text{H}}:m_{\text{D}}:m_{\text{T}}$ to run 1:2:3. The exponents become 2.34 and 3.34 if reduced masses

$$k_{\text{H}}/k_{\text{D}} = (k_{\text{D}}/k_{\text{T}})^{2.26} \quad (12)$$

$$k_{\text{H}}/k_{\text{T}} = (k_{\text{D}}/k_{\text{T}})^{3.26} \quad (13)$$

are used instead.¹⁷ Comparison of $k_{\text{H}}^{\text{H}}/k_{\text{L}}^{\text{H}}$ values in Table II (columns 4 and 8) with values calculated from $k_{\text{D}}^{\text{D}}/k_{\text{T}}^{\text{D}}$ (Table V, columns 7 and 9, respectively) shows that eq 12 and 13 give values that are too low by a margin well outside experimental error when tunneling is important. A similar comparison for the secondary isotope effects (columns 6 and 10 in Table II with columns 8 and 10, respectively, in Table V) shows deviations in the same direction from eq 12 and 13.

Qualitatively, the greater effect of tunneling on the comparison of D/T with H/D or H/T effects than on the comparison of H/D and H/T effects with each other is readily explained. Because of the attenuation of tunneling by increased mass, the relative contribution of tunneling to a D/T isotope effect will be substantially less than to either an H/D or H/T effect. For the first case, both isotopic substrates suffer diminished tunneling, while for the latter two only one does. Thus deviations from eq 11 can be used to detect tunneling in favorable cases, provided the isotopic substrates are chosen so as to maximize the deviation. Most of the deviations persist, incidentally, if reduced masses are used to calculate the exponents in eq 12 and 13.

The smaller contribution of tunneling to D/T than to H/D or H/T isotope effects results, predictably, in more "normal" temperature dependences for the D/T effects. Comparison of column 3 with column 4 and of column 5 with column 6 (Table VI) shows distinctly larger $A_{\text{H}}/A_{\text{L}}$ values for the primary isotope effects calculated from $k_{\text{D}}^{\text{D}}/k_{\text{T}}^{\text{D}}$ values than from the actual $k_{\text{H}}^{\text{H}}/k_{\text{L}}^{\text{H}}$ values in all cases where tunneling is significant ($n_{\text{OH}} = 0.3-0.5$), but

not where tunneling is negligible ($n_{\text{OH}} = 0.9$). The same is true of the secondary effects (Table VI, compare column 7 with column 8 and column 9 with column 10), except that observable differences are now limited to models 4 and 5, where tunneling makes substantial contributions to the secondary isotope effects.

In view of the success of multiple labeling in providing evidence for tunneling contributions to primary and secondary hydrogen isotope effects, the influence of deuteration on carbon isotope effects was next explored. We had previously presented evidence that tunneling can contribute to carbon isotope effects on proton removal from carbon.²²⁻²⁵ The results of the calculations are given in Table IV. The carbon isotope effects for d_0 and d_2 species are compared.

As far as the semiclassical isotope effects are concerned (compare column 3 with column 4 and column 7 with column 8) deuteration clearly raises the carbon isotope effect except for model 1 with $n_{\text{OH}} = 0.1$. The differences are barely large enough to observe for models 1 and 3, though they are substantial for models 4 and 5. The situation is reversed with the full carbon isotope effects (compare column 5 with column 6 and column 9 with column 10). With models 1 and 3 the tunneling contribution just counterbalances the semiclassical effect, and the carbon isotope effects are almost the same for the d_0 and d_2 species. With models 4 and 5, the carbon isotope effects become decisively smaller for the d_2 species at $n_{\text{OH}} = 0.3-0.5$, the region where tunneling is most important. The calculations thus predict that deuteration should raise carbon isotope effects when tunneling is unimportant but lower them when tunneling makes a sizable contribution. In intermediate cases, deuteration should have little or no influence on the carbon isotope effect.

Confirmation of these conclusions can again be sought in the temperature dependences. The A_{12}/A_{13} and A_{12}/A_{14} values (Table VII) are close to unity (0.976-1.009) when tunneling is slight to moderate, as is the case for models 1 and 3 and for all models when $n_{\text{OH}} = 0.9$. When tunneling is important, however, A_{12}/A_{13} can run as low as 0.818 and A_{12}/A_{14} as low as 0.693. Since A_{12}/A_{14} values have been measured to a precision of 0.01-0.05,²² deviations from unity of the magnitude of those shown by models

(21) Subramanian, Rm.; Saunders, W. H., Jr. *J. Phys. Chem.* **1981**, *85*, 1099-1100.

(22) Miller, D. J.; Subramanian, Rm.; Saunders, W. H., Jr. *J. Am. Chem. Soc.* **1981**, *103*, 3519-3522.

(23) Wilson, J. C.; Källson, I.; Saunders, W. H., Jr. *J. Am. Chem. Soc.* **1980**, *102*, 4780-4784.

(24) Banger, J.; Jaffe, A.; Lin, A.-C.; Saunders, W. H., Jr. *J. Am. Chem. Soc.* **1975**, *97*, 7177-7178.

(25) Banger, J.; Jaffe, A.; Lin, A.-C.; Saunders, W. H., Jr. *Faraday Symp. Chem. Soc.* **1975**, *10*, 113-120.

Table V. Primary and Secondary Deuterium and Tritium Isotope Effects Calculated from the Swain-Schaad Relation for HO⁻ + CCH₂CH₂Cl at 45 °C^{a,b}

model	<i>n</i> _{OH}	(<i>k</i> _H ^H / <i>k</i> _D ^H) _{sc} ^{1.44}	(<i>k</i> _H ^H / <i>k</i> _T ^H) ^{1.44}	(<i>k</i> _H ^H / <i>k</i> _D ^H) _{sc} ^{1.44}	(<i>k</i> _H ^H / <i>k</i> _T ^H) ^{1.44}	(<i>k</i> _D ^D / <i>k</i> _T ^D) ^{2.26}	(<i>k</i> _D ^D / <i>k</i> _T ^D) ^{2.26}	(<i>k</i> _D ^D / <i>k</i> _T ^D) ^{3.26}	(<i>k</i> _H ^D / <i>k</i> _T ^D) ^{3.2}
1	0.3	10.300	17.852	1.036	1.039	6.537	1.025	15.002	1.036
	0.5	10.251	16.731	1.070	1.077	6.415	1.048	14.601	1.070
	0.9	2.313	2.320	1.167	1.167	1.828	1.105	2.388	1.154
3	0.3	8.400	13.578	1.046	1.101	5.552	1.048	11.835	1.070
	0.5	8.169	12.389	1.085	1.129	5.343	1.067	11.214	1.098
	0.9	2.174	2.182	1.152	1.152	1.750	1.088	2.242	1.129
4	0.3	7.545	18.229	1.045	1.275	5.941	1.100	13.071	1.147
	0.5	7.415	15.356	1.082	1.296	5.587	1.121	11.962	1.180
	0.9	2.169	2.185	1.162	1.164	1.747	1.097	2.236	1.144
5	0.3	7.253	22.751	1.039	1.411	6.219	1.121	13.963	1.180
	0.5	7.174	17.779	1.076	1.406	5.766	1.146	12.517	1.217
	0.9	2.167	2.187	1.168	1.170	1.744	1.102	2.230	1.151

^{a,b} See corresponding footnotes to Table II.**Table VI.** Ratios of Arrhenius Preexponential Factors for Deuterium and Tritium Isotope Effects for HO⁻ + CCH₂CH₂Cl at 25–55 °C^{a,b}

model	<i>n</i> _{OH}	<i>A</i> _H / <i>A</i> _L ^c from							
		<i>k</i> _H ^H / <i>k</i> _D ^H	(<i>k</i> _D ^D / <i>k</i> _T ^D) ^{2.26}	<i>k</i> _H ^H / <i>k</i> _T ^H	(<i>k</i> _D ^D / <i>k</i> _T ^D) ^{3.26}	<i>k</i> _H ^H / <i>k</i> _D ^H	(<i>k</i> _D ^D / <i>k</i> _T ^D) ^{2.26}	<i>k</i> _H ^H / <i>k</i> _T ^H	(<i>k</i> _D ^D / <i>k</i> _T ^D) ^{3.26}
1	0.3	0.507	0.696	0.432	0.593	0.993	0.994	0.990	1.156
	0.5	0.558	0.711	0.479	0.611	0.981	0.981	0.974	0.974
	0.9	0.879	0.887	0.829	0.814	0.963	0.964	0.952	0.949
3	0.3	0.548	0.700	0.465	0.598	0.938	0.988	0.917	0.982
	0.5	0.602	0.715	0.517	0.616	0.945	0.976	0.921	0.966
	0.9	0.879	0.868	0.830	0.815	0.956	0.977	0.940	0.966
4	0.3	0.149	0.474	0.102	0.340	0.587	0.914	0.481	0.879
	0.5	0.245	0.519	0.175	0.388	0.663	0.912	0.579	0.875
	0.9	0.875	0.861	0.823	0.805	0.958	0.950	0.944	0.939
5	0.3	0.033	0.366	0.019	0.234	0.284	0.856	0.190	0.800
	0.5	0.107	0.430	0.068	0.296	0.440	0.862	0.335	0.807
	0.9	0.873	0.857	0.819	0.801	0.965	0.966	0.947	0.943

^{a,b} See corresponding footnotes to Table II. ^c Ratio of Arrhenius preexponential factors for protium (H) and deuterium or tritium (L).**Table VII.** Ratios of Arrhenius Preexponential Factors for β-¹³C and β-¹⁴C Isotope Effects for HO⁻ + CCH₂CH₂Cl at 25–55 °C^{a,c}

model	<i>n</i> _{OH}	<i>A</i> ₁₂ / <i>A</i> ₁₃ from		<i>A</i> ₁₂ / <i>A</i> ₁₄ from	
		<i>k</i> _H ^H / <i>k</i> _{H(13)} ^H	<i>k</i> _D ^D / <i>k</i> _{D(13)} ^D	<i>k</i> _H ^H / <i>k</i> _{H(14)} ^H	<i>k</i> _D ^D / <i>k</i> _{D(14)} ^D
1	0.3	0.9983	1.0020	0.9984	1.0082
	0.5	0.9869	0.9995	0.9758	0.9997
	0.9	1.0004	0.9963	1.0012	0.9934
3	0.3	0.9912	1.0001	0.9835	1.0004
	0.5	0.9777	0.9946	0.9592	0.9903
	0.9	1.0011	0.9972	1.0026	0.9952
4	0.3	0.9236	0.9885	0.8625	0.9772
	0.5	0.9002	0.9776	0.8247	0.9591
	0.9	0.9885	1.0004	1.0083	1.0012
5	0.3	0.8183	0.9786	0.6927	0.9595
	0.5	0.8192	0.9669	0.6960	0.9397
	0.9	1.0045	1.0019	1.0091	1.0023

^{a,b} See corresponding footnotes to Table II. ^c See corresponding footnote to Table IV.

4 and 5 should be easy to detect. Deuteration suppresses tunneling to a sufficient extent to produce marked increases in *A*₁₂/*A*₁₃ and *A*₁₂/*A*₁₄ (compare column 3 with column 4 and column 5 with column 6).

A relationship between ¹³C and ¹⁴C isotope effects analogous to eq 11–13 for deuterium and tritium isotope effects can be derived (eq 14).^{26–28} Application of this equation to the results

$$k_{12}/k_{14} = (k_{12}/k_{13})^{1.9} \quad (14)$$

in Table IV reveals, unfortunately, no deviations due to tunneling of sufficient magnitude for reliable experimental detection.

The results of the present calculations bear on the range of applicability of the rule of the geometric mean.²⁹ The principle behind the rule is that the isotope effect for a doubly labeled species should, to a good approximation, be the product of the isotope effects for the corresponding singly labeled species. For 2, for example, eq 15 should hold. Simple algebra shows that this will

$$k_{\text{H}}^{\text{H}}/k_{\text{D}}^{\text{D}} = (k_{\text{H}}^{\text{H}}/k_{\text{H}}^{\text{D}})(k_{\text{H}}^{\text{H}}/k_{\text{D}}^{\text{H}}) \quad (15)$$

be the case only if $k_{\text{H}}^{\text{H}}/k_{\text{H}}^{\text{D}} = k_{\text{H}}^{\text{H}}/k_{\text{D}}^{\text{D}}$, which comparison of column 6 of Table II and column 4 of Table III shows *not* to be true when tunneling is important. Thus, the rule can be expected to fail if isotopic substitution in one position affects the contribution of tunneling to the kinetic isotope effect at another.

Summary

Until recently, the only experimental criteria for tunneling in slow proton transfers were unusually high primary hydrogen isotope effects and/or unusually low *A*_H/*A*_L values (L = D or T) for these effects. The present calculations, along with recent experiments and calculations cited above, have made substantial additions to the number of tools available to the chemist interested in exploring the role of tunneling. These can be summarized as (1) the magnitude and temperature dependence of secondary deuterium and tritium isotope effects, (2) deviations from the predicted relations (eq 12 and 13) between D/T and either H/D or H/T isotope effects, both primary and secondary, (3) the differing temperature dependences of directly measured H/D and H/T isotope effects as compared to those calculated from D/T isotope effects, and (4) the effect of deuteration on the magnitude and temperature dependence of *k*₁₂/*k*₁₃ and *k*₁₂/*k*₁₄.

The predictions in this paper are derived from a specific set of simplified models and from the Bell treatment of the tunnel effect. The bases of the predictions, however, are the expectations

(26) Reference 15, pp 52–54 and 74–75.

(27) Bigeleisen, J. *J. Chem. Phys.* **1952**, *56*, 823–828.(28) Stern, M. J.; Vogel, P. C. *J. Chem. Phys.* **1971**, *55*, 2007–2013.(29) Bigeleisen, J. *J. Chem. Phys.* **1955**, *23*, 2264–2267.

that tunneling probability should depend on the effective mass along the reaction coordinate and that increased tunnel corrections should steepen the apparent temperature dependences of isotope effects.³⁰ These ideas are not dependent on the details of any

specific model, so the predictions can reasonably be expected to apply in a qualitative sense to any thermally activated slow hydrogen transfers.

Registry No. ¹³C, 14762-74-4; ¹⁴C, 14762-75-5; deuterium, 7782-39-0; tritium, 10028-17-8.

(30) References 11, pp 63-67.

An Unusual C-C Bond Cleavage in a Bulky Metal Alkoxide: Syntheses and X-ray Crystal Structures of Three-Coordinate Mn(II) and Cr(II) Complexes Containing the Di-*tert*-butylmethoxide Ligand

Brendan D. Murray, Håkon Hope, and Philip P. Power*

Contribution from the Department of Chemistry, University of California, Davis, California 95616. Received April 5, 1984

Abstract: Two multinuclear alkoxides containing the di- or tri-*tert*-butylmethoxide ligand have been characterized by X-ray diffraction. The molecular structures of $[\text{Cr}(\mu\text{-OCH-}t\text{-Bu}_2)(\text{OC-}t\text{-Bu}_3)_2]$ (**1**) and $[\text{Mn}_3(\text{OCH-}t\text{-Bu}_2)_6]$ (**3**) both contain the *t*-Bu₂CHO⁻ group acting as a bridging ligand. The crystal data (Mo K α , $\lambda = 0.71069 \text{ \AA}$) at 140 K are as follows. **1**: $a = 8.151(2) \text{ \AA}$, $b = 16.520(4) \text{ \AA}$, $c = 17.434(4) \text{ \AA}$, $\alpha = 94.46(2)^\circ$, $\beta = 93.94(2)^\circ$, $\gamma = 101.01(2)^\circ$, $Z = 2$ (dimers), space group $P\bar{1}$. **3**: $a = 12.092(2) \text{ \AA}$, $b = 21.868(4) \text{ \AA}$, $c = 22.748(4) \text{ \AA}$, $\beta = 96.57(2)^\circ$, $Z = 4$, space group $P2_1/c$. For **1**, $R = 0.050$; for **3**, $R = 0.048$. The geometry at the chromium atoms in **1** is distorted trigonal planar. Complex **3** is the first homoleptic manganese(II) alkoxide to be structurally characterized. The nonlinear trimer has a Mn-Mn-Mn angle of 154.0° and does not possess any formal Mn-Mn bonds. Both complexes exhibit very wide M-O-C angles at the terminal alkoxides. In complex **1** the Cr-O-C_{terminal} moiety is essentially linear. The di-*tert*-butylmethoxide ligand in **1** results from an unusual C-C bond cleavage under mild conditions in the complex $[\text{Cr}(\text{OC-}t\text{-Bu}_3)_2\text{LiCl}(\text{THF})_2]$ (**2**).

Recent years have seen a renewed interest in the synthesis and chemical properties of alkoxide and aryloxo complexes.¹⁻¹¹ Most transition-metal alkoxide and aryloxides containing smaller ligands such as OMe⁻, OEt⁻, or OPh⁻ are oligomeric.⁴ This is due to the excellent bridging ability and lower steric requirements of the alkoxo group compared to isoelectronic amido or alkyl substituents. In sharp contrast, some recent reports have concentrated on the use of bulky aryloxo groups (e.g., 2,6-di-*tert*-butyl-4-methylphenoxide) to achieve low coordination numbers in complexes involving main group, transition, or lanthanoid metals.^{5-9,11} These complexes are in general monomeric and exhibit low coordination (typically three) at the metal.

An interesting consequence of the severe steric requirements imposed by the larger alkoxo groups has been the discovery of

reactions involving C-H bond activation and the formation of benzyne intermediates not seen with the smaller substituents.^{8,9} In addition, work in this laboratory with the large tri-*tert*-butylmethoxide ligand, *t*-Bu₃CO⁻, has allowed the synthesis of the first structurally characterized examples of monomeric alkoxide complexes for Cr(II) and Mn(II).^{1,2}

Recently we reported that the green complex $[\text{Cr}\{\text{OC-}t\text{-Bu}_3\}_2\text{LiCl}(\text{THF})_2]$ is formed when CrCl₃ is treated with *t*-Bu₃COLi in Et₂O/THF solution.¹ When it is dissolved in warm hexane, LiCl is precipitated and a blue-green crystalline complex is obtained. The complex gave a C, H elemental analysis consistent with the formulation $[\text{Cr}(\text{OC-}t\text{-Bu}_3)_2(\text{THF})_2]$.¹² This composition seemed reasonable since complexes of the type $[\text{Cr}(\text{OR})_2(\text{THF})_2]$ (where OR is 2,6-di-*tert*-butylphenolate or 2,4,6-tri-*tert*-butylphenolate)⁶ and *trans*- $[\text{Cr}\{\text{N}(\text{SiMe}_3)_2\}_2(\text{THF})_2]$ had been reported.¹³

However, upon GC/MS analysis of the filtrate we were surprised by the high concentration of C₄H₈ (mostly isobutene) present. In order to explain the origin of C₄H₈ we determined the structure of the blue-green complex.

In this paper we describe the first structural characterization of (i) a three-coordinate chromium(II) dimer, $[\{\text{Cr}(\mu\text{-OCH-}t\text{-Bu}_2)(\text{OC-}t\text{-Bu}_3)_2\}]$ (**1**), which contains only alkoxide ligands, and (ii) a homoleptic manganese(II) alkoxide trimer, $[\text{Mn}_3(\text{OCH-}t\text{-Bu}_2)_6]$. Both of these complexes have the di-*tert*-butylmethoxide group acting as a bridging ligand. The blue-green complex **1** is the result of an unusual solvent dependent C-C cleavage from the compound $[\text{Cr}\{\text{OC-}t\text{-Bu}_3\}_2\text{LiCl}(\text{THF})_2]$ (**2**).

(1) Hvoslief, J.; Hope, H.; Murray, B. D.; Power, P. P. *J. Chem. Soc., Chem. Commun.* **1983**, 1438-1439.

(2) Murray, B. D.; Power, P. P. *J. Am. Chem. Soc.* **1984**, *106*, 7011-7015.

(3) Bochmann, M.; Wilkinson, G.; Young, G. B.; Hursthouse, M. B.; Malik, K. M. A. *J. Chem. Soc., Dalton Trans.* **1980**, 1863-1871.

(4) Bradley, D. C.; Mehrotra, R. C.; Gaur, D. P. "Metal Alkoxides"; Academic Press: London, 1978.

(5) Horvath, B.; Mosler, R.; Horvath, E. G. *Z. Anorg. Allg. Chem.* **1979**, *449*, 41-51.

(6) Horvath, B.; Horvath, E. G. *Z. Anorg. Allg. Chem.* **1979**, *457*, 51-61.

(7) Cetinkaya, B.; Hitchcock, P. B.; Lappert, M. F.; Torroni, S.; Atwood, J. L.; Hunter, W. E.; Zaworotko, M. J. *J. Organomet. Chem.* **1980**, *188*, C31-C35.

(8) Chamberlain, L.; Keddington, J.; Rothwell, I. P.; Huffman, J. C. *Organometallics* **1982**, *1*, 1538-1540.

(9) Chamberlain, L. R.; Rothwell, I. P. *J. Am. Chem. Soc.* **1983**, *105*, 1665-1666.

(10) Chisholm, M. H.; Cotton, F. A.; Extine, M. W.; Rideout, D. C. *Inorg. Chem.* **1978**, *18*, 120-125.

(11) Hitchcock, P. B.; Lappert, M. F.; Singh, A. *J. Chem. Soc., Chem. Commun.* **1983**, 1499-1501.

(12) The C, H elemental analysis is also consistent with the dimer $[\{\text{Cr}(\mu\text{-OCH-}t\text{-Bu}_2)(\text{OC-}t\text{-Bu}_3)_2\}]$.

(13) Bradley, D. C.; Hursthouse, M. B.; Newing, C. W.; Welch, A. J. *J. Chem. Soc., Chem. Commun.* **1972**, 567-568.